
Article:
Dharmaprani, D., Jenkins, E.V., Quah, J.X. et al. (10 more authors) (2022) A governing equation for rotor and wavelet number in human clinical ventricular fibrillation: Implications for sudden cardiac death. Heart Rhythm, 19 (2). pp. 295-305. ISSN 1547-5271

https://doi.org/10.1016/j.hrthm.2021.10.008

A governing equation for rotor and wavelet number in human clinical ventricular fibrillation: Implications for sudden cardiac death

Dhani Dharmaprani[1,2], Evan V. Jenkins[1], Jing X. Quah[1,3], Anandaroop Lahiri[3], Kathryn Tiver[3], Lewis Mitchell[4], Christopher P. Bradley[5], Martin Hayward[6,7], David J. Paterson[8], Peter Taggart[9], Richard H. Clayton[10], Martyn P. Nash[5], Anand N. Ganesan[1,3].

From:

1. College of Medicine and Public Health, Flinders University, Adelaide, Australia
2. College of Science and Engineering, Flinders University, Adelaide, Australia
3. Department of Cardiovascular Medicine, Flinders Medical Centre, Australia
4. School of Mathematical Sciences, University of Adelaide, Australia
5. Auckland Bioengineering Institute, University of Auckland, New Zealand
6. University College London Hospitals NHS Foundation Trust, London, UK
7. UCLH Department of Cardiothoracic surgery, London, UK
8. Department of Physiology, Anatomy and Genetics, University of Oxford, UK
9. Institute of Cardiovascular Science, University College London, UK
10. Insigneo Institute for in silico Medicine, University of Sheffield, UK.

Correspondence:

Dr Anand Ganesan

Flinders University and Flinders Medical Centre, Adelaide, Australia

anand.ganesan@flinders.edu.au

Word count: 6925 (including acknowledgments, data sharing plans, introduction, methods, results, discussion, references, figures and tables)

Published in Heart Rhythm https://doi.org/10.1016/j.hrthm.2021.10.008

ABSTRACT

Rationale

Ventricular fibrillation (VF) is characterised by multiple wavelets and rotors. No equation to predict the number of rotors and wavelets observed during fibrillation has been validated in human VF.

Objective

We hypothesized a single equation derived from a Markov M/M/∞ birth-death process, could predict the number of rotors and wavelets occurring in human clinical VF.

Methods

Epicardial induced VF (256-electrodes) recordings obtained from patients undergoing cardiac surgery were studied (n=12 patients, n=62 epochs). Rate constants for phase singularity (PS, which occur at the pivot points of rotors) and wavefront (WF) formation and destruction were derived by fitting distributions to PS and WF inter-formation and lifetimes. These rate-constants were combined in an M/M/∞ governing equation to predict the number of PS and WF in VF episodes. Observed distributions were compared to those predicted by the M/M/∞ equation.

Results

The M/M/∞ equation accurately predicted average PS and WF number and population distribution, demonstrated in all epochs. Self-terminating episodes of VF were distinguished from VF episodes requiring termination by a trend towards slower PS destruction, and slower rates of PS formation, and a slower mixing rate of the VF process, indicated by larger values of the second-largest eigenvalue modulus (SLEM) of the M/M/∞ birth-death matrix. The longest-lasting PS (associated with rotors) had shorter inter-activation time intervals compared to shorter lasting PS lasting <150 ms (~1 PS rotation in human VF).

Conclusions

The M/M/∞ equation explains the number of wavelets and rotors observed, supporting a paradigm of VF based on statistical fibrillatory dynamics.

Keywords

Ventricular fibrillation, rotors, wavelets, mechanisms, phase singularities, renewal process

INTRODUCTION

Ventricular fibrillation (VF) is a condition that occurs when the normally synchronised rhythm of the heart breaks down in the heart's two bottom chambers, causing the heart to beat in a rapid and erratic manner.[1] VF is the leading cause of sudden cardiac death.[2] This lethality has made it difficult to study the mechanisms responsible for causing and sustaining VF[3 4]

Although several theories have been put forward, the mechanisms underlying VF remain incompletely understood.[4] Classical hypotheses for the VF mechanism include the multiple-wavelet and rotor theories[4-6], but these theories do not offer a governing equation to predict the number of rotors or wavelets likely to be observed during a VF episode.

Recently, we developed such a governing equation to study the population dynamics of rotors and wavelets in atrial fibrillation (AF).[7] We demonstrated that the formation and destruction of rotors and wavelets could be characterized by rate constants λ_f and λ_d, and that these could be combined in an M/M/∞ birth-death process to develop stationary state equations to predict the number and population distribution of rotors and wavelets. We therefore hypothesized that the previously developed governing equation could similarly be applied to human clinical VF to explain the population dynamics of rotors and wavelets.

METHODS

Theory – Explanation of the origin of the M/M/∞ birth-death equation

This section explains the background for the proposed VF governing equation (Schematic provided in Figure 1). This theory was then applied to human VF recordings.

Human VF is characterized by spatiotemporally disordered wave propagation, with repetitive regeneration of rotors and wavelets. Reasoning from the intrinsic spatiotemporal disorder of fibrillation, we hypothesize that individual formation and destruction events of phase singularities (PS) and wavefronts (WF) (which occur at the pivot of rotors/the free-ends of wavelets, and depict the front of an excitation wave respectively, Figure 1) may be effectively statistically independent, and therefore converge to predictable rates.[7, 8] This gives rise to exponential or '*Markovian*' PS and WF inter-event time distributions.[7, 8] For PS and WF lifetimes (time taken for PS or WF to die) this distribution is given by:

$$f(t) = \{\lambda_d \mathrm{e}^{-\lambda_d \mathrm{t}} \quad t \geq 0\} \ (1)$$

where t is time, and PS λ_d the PS destruction rate, and WF λ_d the WF destruction rate .[8]

Similarly, PS and WF inter-formation time distribution (time between consecutive new PS or WF formations) is given by:

$$f(t) = \left\{\lambda_f \mathrm{e}^{-\lambda_f \mathrm{t}} \quad t \geq 0\right\} \ (2)$$

where t is time, and PS λ_f the PS formation rate, and WF λ_f the WF formation rate .[8]

Here, we further hypothesized that PS and WF λ_f and λ_d could be combined in an M/M/∞ birth-death process to develop a governing equation to model the population distribution of rotors and wavelets in VF. An M/M/∞ birth-death process is a continuous-time Markov chain used when new events have a Markovian rate of arrivals and destruction (denoted by 'M').[7] The ∞ denotes the concept that new PS or WF are potentially

immediately available for destruction as soon as they are formed. (S1). The governing M/M/∞ equation gives the probability (P_n) of having a population size n of PS or WF[9]:

$$P_n = \frac{\left(\lambda_f / \lambda_d\right)^n e^{-\lambda_f / \lambda_d}}{n!} \quad (3)$$

The average number (N) of PS or WF is summarized using the expectation of the governing M/M/∞ equation[9]:

$$N = \frac{\lambda_f}{\lambda_d} \quad (4)$$

where λ_f and λ_d are either the rates of PS or WF formation and destruction respectively. We have previously shown an M/M/∞ birth-death process could model PS and WF population dynamics in AF.[7]

As a further means of gaining insight into the population dynamics of rotors and wavelets, we studied the M/M/∞ Markov transition matrix properties. A key property of this transition matrix is the '*mixing rate*', which represents the time taken to reach the stationary state distribution, expressed in terms of the interaction of the formation process (governed by PS or WF λ_f) and the destruction process (governed by PS or WF λ_d). The mixing rate is specifically given by[10]:

$$Mixing\ rate = \log(1 - z) \quad (5)$$

where z is the second largest eigenvalue modulus (or SLEM) of the Markov transition matrix (S7). In this study, we specifically hypothesized that VF termination would occur due to a deviation from the stationary state of VF dynamics, due to this distribution being reached more slowly (reflected by a slower mixing rate).[7]

Human clinical VF recordings

The human VF study is as described by Nash et al. [4] The study recruited patients

144 undergoing routine coronary bypass graft procedures for ischemic heart disease with cross-
145 clamp fibrillation. These studies were approved by the Hospital Ethics Committee (REC
146 01/0130), and informed consent obtained. Individual patient details are given in Supplemental
147 Table 1 (S2). During the procedure, cardiopulmonary bypass was instituted, and VF induced
148 using 50Hz burst pacing. 30 seconds of control VF was recorded with myocardial perfusion,
149 and the aorta then cross-clamped to achieve global myocardial ischemia. After 150 seconds,
150 the cross-clamp was removed to allow coronary reflow, and a further 30 seconds recorded
151 before defibrillation. We compared the characteristics of sustained episodes, which lasted the
152 full 210 seconds of recording, to episodes which self-terminated spontaneously without
153 requiring defibrillation.

154 Recordings were obtained using a 256-electrode epicardial sock (interelectrode
155 spacing-10 mm) fitted over the ventricles.[4] Unipolar epicardial electrograms were sampled at
156 1kHz (UnEmap system, Uniservices Ltd, New Zealand) and preprocessed as previously
157 described.[4, 7, 8] To allow for phase singularity (PS) and wavefront (WF) detection, 3-
158 dimensional mesh vertices were mapped onto a 2D polar plot using a cone-shaped surface
159 projection and Delaunay triangulation (S3).[4] Electrode potentials were linearly interpolated
160 onto a fine regular 2-dimensional grid (100x100 points), and instantaneous phase calculated
161 using the Hilbert transform (S4).[8]

162 PS and WF detection were performed using a previously established algorithm (S5).[4]
163 New PS were defined as the detection of a PS not falling within the surrounding electrode
164 neighborhood of radius 8mm of another PS for a duration >10ms. As a sub-group analysis,
165 PS lasting >200ms (to ensure at least 1 full rotation period) were separately analyzed.
166 Wavelets were detected by identifying lines of zero phase. A graph theory approach was
167 used to identify new wavelets, as well as track wavelet splitting and merging events (S5).[7, 11]

Statistical analysis

PS and WF tracking was used to calculate PS & WF lifetimes (times taken for PS or WF to die) and inter-formation times (times between consecutive PS or WF formations). Modelling of PS and WF inter-formation times and lifetimes distributions was performed using a maximum likelihood approach, using an automated model selection method based on the Akaike Information Criterion (AIC) (S6). As confirmation, a chi-squared (χ^2) goodness of fit statistic was used to verify the conformance of λ_f and λ_d with an exponential-type distribution. The autocorrelation of PS and WF lifetimes and inter-formation times was also assessed to verify statistical independence (S8).

To test the hypothesis that the number and population distribution of PS/ WF could be predicted by the governing equation, the average number and population distribution calculated using the equation was compared to that directly observed using bivariate Pearson's correlation, and a chi-squared (χ^2) goodness of fit statistic (accepted significance suggesting a good fit at α>0.05).

To understand the differences in renewal process characteristics between self-terminating and sustained VF episodes, λ_f, λ_d and the mixing rate in sustained VF episodes were compared to those from spontaneously terminating VF episodes using an independent samples t-test with P<0.05 indicating significant differences. Mean dominant frequency (DF) and VF cycle length (CL) in sustained versus spontaneously terminating VF episodes were also studied using independent samples t-tests (S9).

To evaluate the effect of VF progression, we studied how the parameters λ_f and λ_d evolved i) through different stages of perfused VF, ischemia and reflow, and ii) temporally as each VF episode progressed over time. Specifically, we used generalized linear mixed effects models to study changes in λ_f and λ_d (set as the target variable) when either stage (perfusion, ischemia and reflow), or time was set as the fixed effect respectively. Specifically,

we reasoned that the use of 5-sec windows allows an increase in the temporal resolution of the changes occurring for λ_f and λ_d.

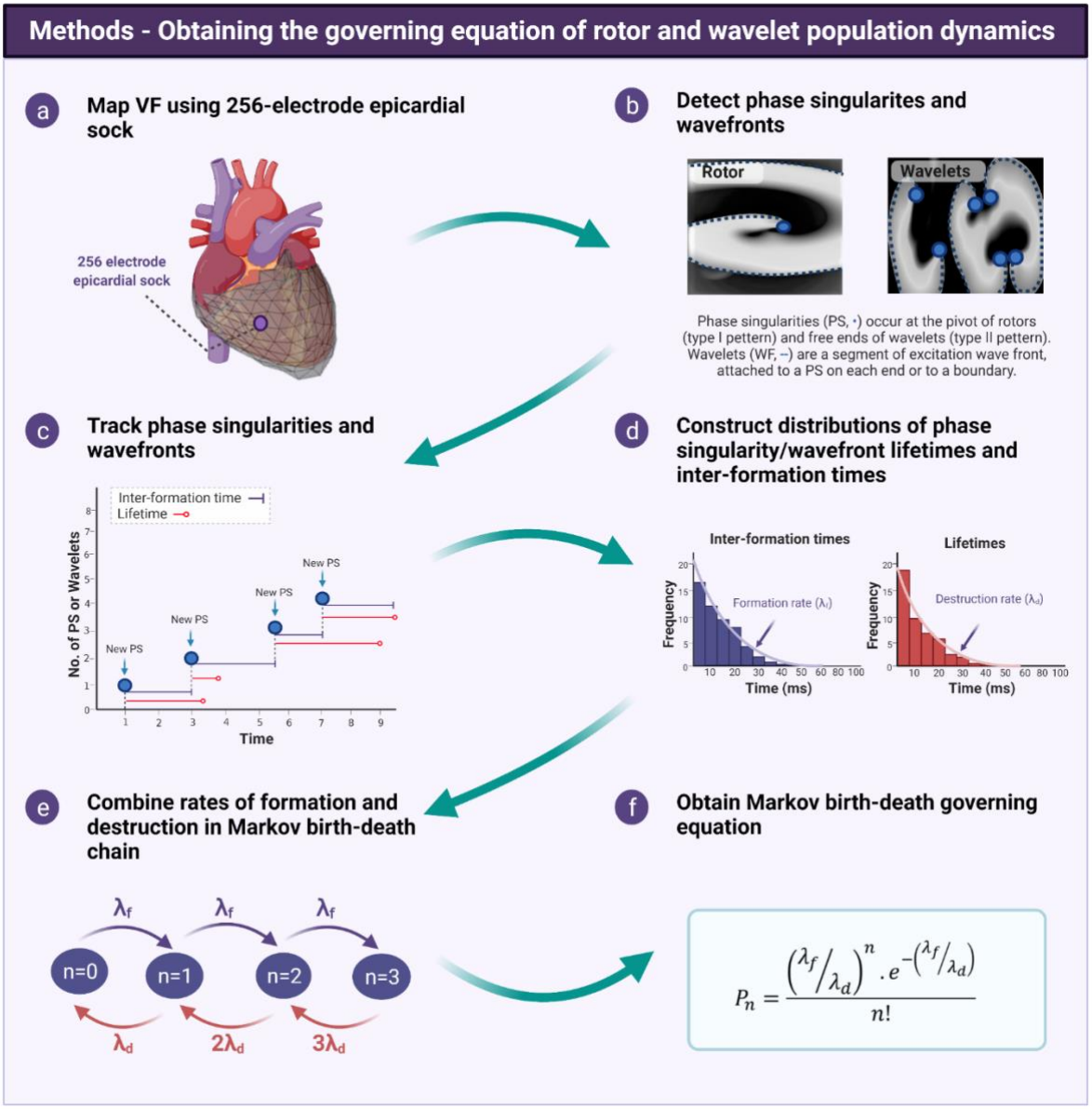

Figure 1: Methods – Obtaining the governing equation of rotor and wavelet population dynamics for human clinical VF data

To develop a governing equation of rotor and wavelet population dynamics, VF was mapped using a 256-elctrode sock (**1A**), and phase singularities (PS) and wavefronts (WF) were detected using phase mapping **(1B**). PS and WF were tracked to measure their lifetimes and inter-formation times (**1C**). Distributions were constructed from PS and WF lifetimes (times taken for PS and WF to die) and inter-formation times (times between new consecutive PS or WF formations) and fit using maximum likelihood fitting and Akaike Information Criterion to: i) determine the underlying type of birth-death process and ii) measure rates of PS and WF formation and destruction (**1D**). Rates of formation and destruction are combined in a Markov birth-death chain modelled by the type of birth-death process underlying PS and WF formation and destruction (**1E**) to produce the governing equation of PS and WF dynamics (**1F**).

RESULTS

Identifying the type of birth-death process underlying PS formation and destruction

PS lifetimes fit to an exponential distribution over all stages of VF

To identify the type of birth-death process underlying PS destruction, PS lifetimes were fit to a range of test distributions and the AIC measured (summary in Supplemental table 2, S11) in n=12 patients (n=8 sustained VF, 56 epochs; n=4 self-terminating VF, 6 epochs) over perfusion, ischemia and reflow stages. The most consistent fit was found to be the exponential (i.e. Markovian), with renewal rate parameter PS λ_d (all cases mean PS λ_d: 0.0097 (95%CI,0.0079,0.0115)), ischemia (mean PS λ_d: 0.0098 (95%CI,0.0095,0.10)) and reflow (mean PS λ_d: 0.0103 (95%CI,0.0097,0.0109) (Supplemental table 2, S11). Example distributions from a single patient are shown in Figure 2A-C.

PS inter-formation times fit to an exponential distribution over all VF stages

PS inter-formation times consistently fit to the exponential (Supplemental Table 2, S121) in n=12 patients over all VF stages. Figures 3D-F demonstrate example PS inter-formation time distributions from a single patient over perfusion, ischemic and reflow stages respectively, which are consistent with an exponential (Supplemental table 2, S11). The mean rate parameter PS λ_f for all patients during perfusion was 0.0172 (95%CI 0.0153,0.0190), ischemia 0.0185 (95%CI,0.0176,0.0194), and reflow 0.0198 (95%CI, 0.0183, 0.213) (Supplemental table 2, S11).

Distributions of phase singularity inter-formation times and lifetimes best fit to the exponential distribution

Distribution fitting over various stages of VF - PS lifetimes

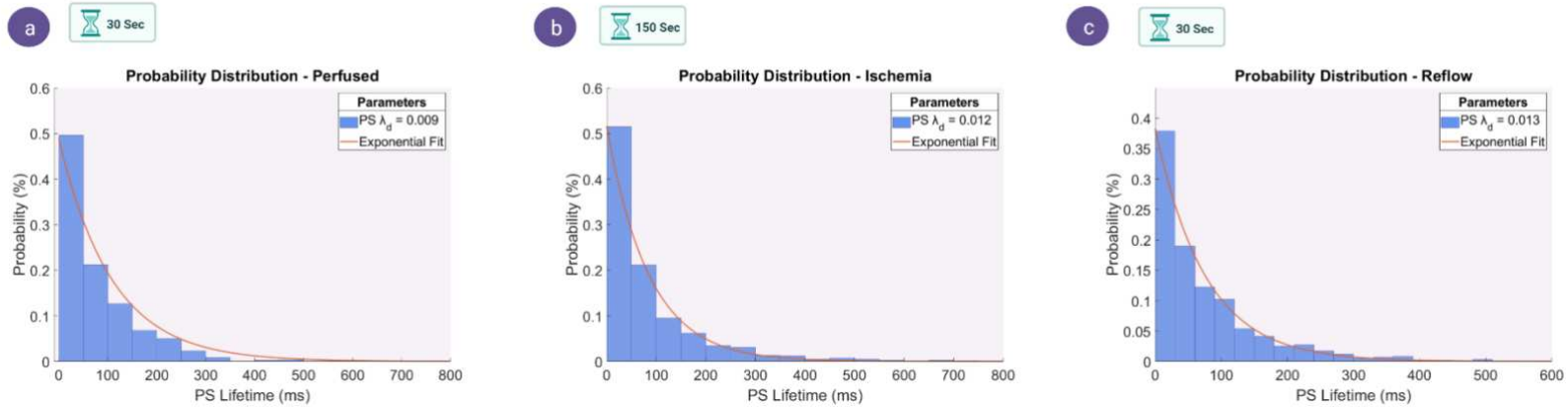

Distribution fitting over various stages of VF - PS inter-formation times

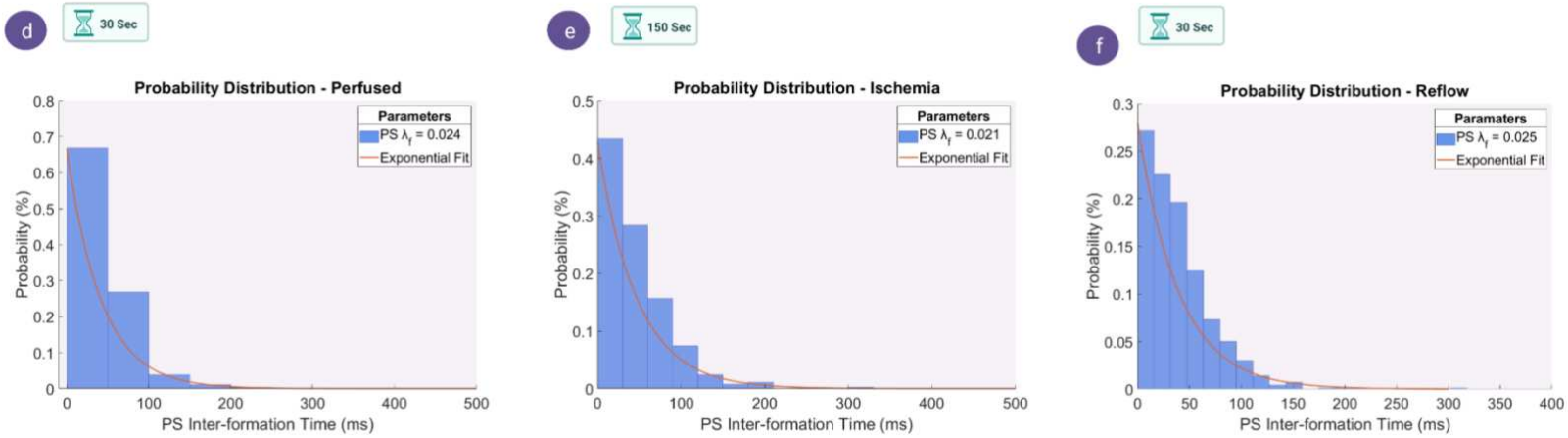

Figure 2: Fitting of PS inter-formation time and lifetime distributions in human clinical VF data was consistent with underlying Markovian processes

(**2A-C**) PS lifetimes were consistent with an exponential distribution over perfusion, ischemia and reflow stages (χ^2 P>0.05, indicating a good fit), consistent them arising from an underlying Markov process. Distributions shown were constructed with a single example 30 second epoch during perfusion, ischemia (first 30secs) and reflow. (**2D-F**) PS inter-formation time distributions were also consistent with an exponential over all stages (χ^2 P>0.05), which exhibits the 'Markovian' property.

M/M/∞ governing equation predicts PS population dynamics in human sustained VF

Figures 3A-C show the predicted average and observed PS number were correlated in all sustained VF epochs (R^2=0.98; P<0.001). Predicted PS population distributions, shown in purple, were compared to the observed population distribution of PS, shown in grey (examples Figure 3D-F), with χ^2 goodness-of-fit-test demonstrating close matching in all epochs (χ^2 P>0.05 all sustained cases, summary in Supplemental table 4, S13). A greater probability of seeing fewer PS was observed at the beginning of the VF episode (perfusion), versus the end of the recording (reflow).

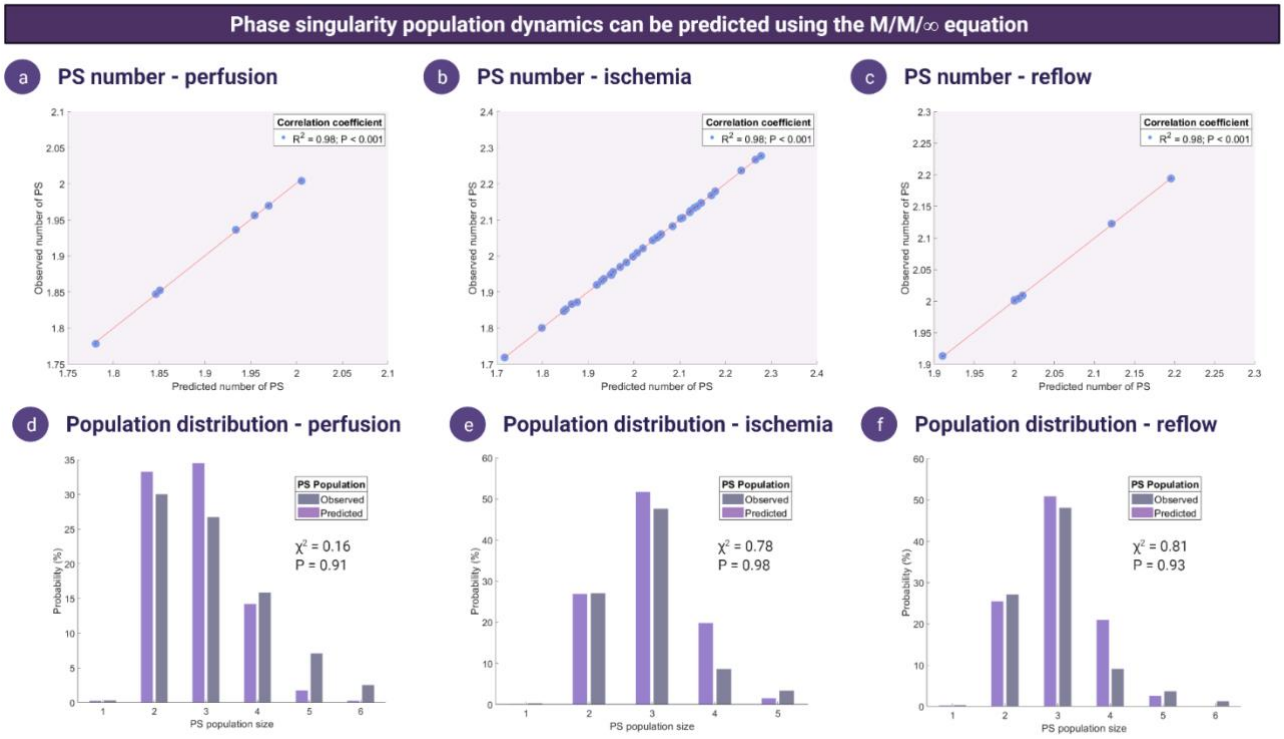

Figure 3: Phase singularity population dynamics can be predicted using the M/M/∞ equation in human clinical VF data

(**3A-C**) Predicted versus observed PS number are highly correlated (R^2=0.98) in epochs and stages of VF (examples shown for a single 30sec epoch during perfusion, ischemia (first 30secs) and reflow stages). This suggests that the governing equation accurately summarises the average PS number observed in VF. (**3D-F**) Predicted PS population distributions fit to observed PS population distributions, with χ^2 P>0.05, indicating a good fit.

M/M/∞ governing equation predicts population dynamics of more sustained PS with lifetimes > 200ms

An important consideration is whether the governing equation would apply to longer-lasting PS, arising from spiral waves where at least 1 full rotation should have occurred. To distinguish this subgroup, we repeated analyses on PS with lifetimes >200ms (to ensure that at least 1 full rotation period had been completed). We showed that for this subgroup, inter-formation times (mean χ^2 p-value perfused = 0.18 (95%CI,0.03,0.39); ischemia = 0.88 (95%CI,0.007,0.17); reflow = 0.06(95%CI,0.011,0.25)) and lifetimes (mean χ^2 p-value perfused = 0.16 (95%CI,0.02,0.34); ischemia = 0.08 (95%CI,0.05,0.16); reflow = 0.06(95%CI,0.011,0.21) processes also consistently fit to the exponential.

Observed PS population distributions also closely matched those predicted by the M/M/∞ governing equation (example Figure 4) with χ^2 goodness-of-fit-testing demonstrating close matching (χ^2 P>0.05 all sustained cases, summary in Supplemental table 5, S14).

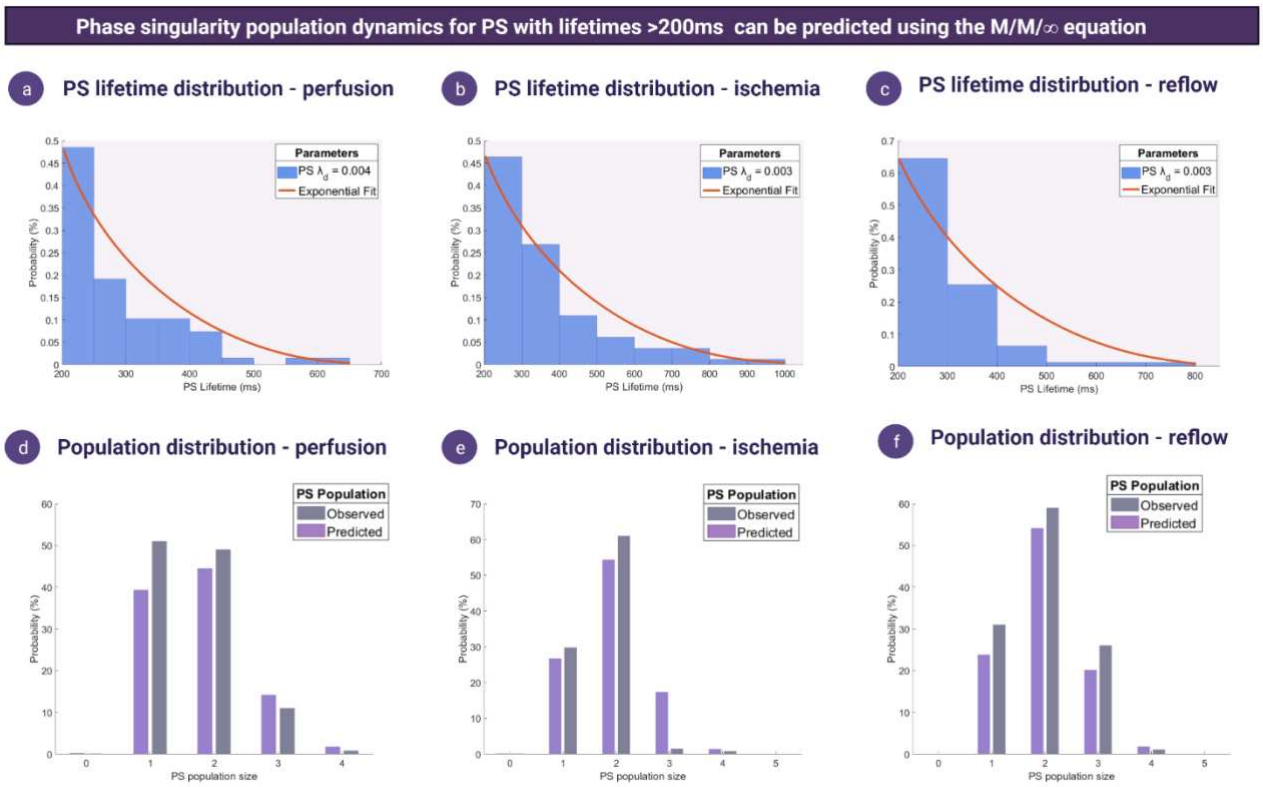

Figure 4: Phase singularity population dynamics for PS with lifetimes >200ms can be predicted using the M/M/∞ equation

(**4A-C**) PS lifetime distributions for PS with lifetimes >200ms generate exponential distributions (examples shown for a single 30sec epoch during perfusion, ischemia (first 30secs) and reflow stages). (**4D-F**) Predicted PS population distributions fit to observed PS population distributions, with χ^2 P>0.05, indicating a good fit.

M/M/∞ governing equation predicts WF population dynamics

Analyses were repeated in all epochs of VF for wavefronts (WF) to further assess the application of the M/M/∞ governing equation. WF inter-event distributions fit best to the exponential indicated by the AIC (Supplemental table 3, S10). Renewal rate constants WF λ_f and WF λ_d were given by the exponential rate parameter, which were combined in the M/M/∞ equation to predict WF population dynamics. Mean WF λ_f in sustained VF cases for perfusion was 0.192 (95%CI,0.128,0.256), 0.240 (95%CI, 0.201,0.274) for ischemia, and 2.96 (95%CI,0.220,0.372) for reflow. Mean WF λ_d in sustained VF cases was 0.0748 (95%CI,0.0569,0.0.748) for perfused VF, 0.0833 (95%CI,0.0745,0.0921) for ischemia, and 0.985 (95%CI,0.0757,1.121) for reflow. The predicted average and observed WF number were highly correlated (R^2 > 0.99; Figure 5C-E) and predicted WF population distributions fit to observed distributions with χ^2 P>0.05 in all epochs (summary in Supplemental table 5, S15) (Figure 5F-H).

When compared to PS λ_f in sustained cases of VF all stages (perfusion, ischemia and reflow), WF λ_f was significantly higher (P<0.001), suggesting higher rates of WF formation. However, PS λ_f and WF λ_f were correlated (R=0.61). Similar results were seen for WF λ_d when compared to PS λ_d, with WF λ_d being significantly faster (P<0.001) and indicating higher rates of WF formation. WF λ_d and PS λ_d were also correlated (R=0.59).

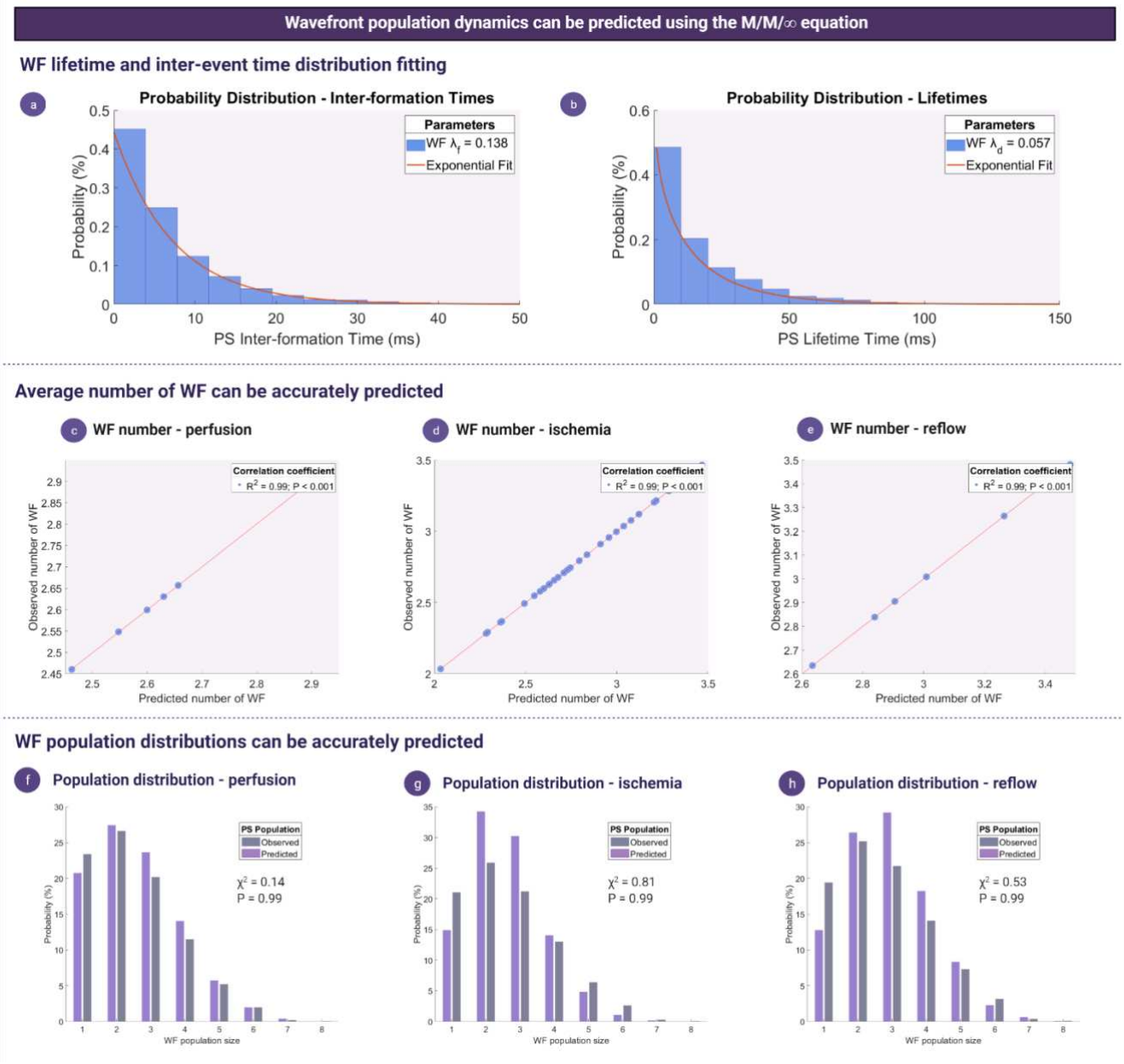

Figure 5: Wavefront population dynamics can be predicted using the M/M/∞ equation in human clinical VF data

(**5A-B**) WF inter-formation and lifetime distributions fit best to the exponential. (**5C-E**) Predicted versus observed WF number are highly correlated in all epochs and over all stages of VF (R^2>0.99 all epochs). (**5F-H**) Predicted WF population distributions fit to observed WF distributions (P > 0.05).

Spontaneous VF termination is associated with slower birth-death mixing rates in human clinical VF data, but not with mean DF or cycle length

When compared in sustained VF episodes (n=56 episodes from n=8 patients), PS λ_f was higher than in spontaneously terminating episodes (n=6 terminating episodes arising from n=5 patients) (P=0.011, Figure 6A). PS λ_d was also higher in sustained VF episodes than in spontaneously terminating episodes, but differences were not statistically significant (P=0.12, Figure 6B). WF λ_f was and WFλ_d were also higher in spontaneously terminating episodes than in self-terminating episodes of VF (WF λ_f P=0.003; WF λ_d P<0.001; Figure 6C-D).

The second-largest eigenvalue modulus (SLEM, Supp S1) of termination cases was consistently higher (mean: 0.9912 (95%CI,0.9888,0.9935) than sustained VF cases (mean: 0.9879 (95%CI,0.9858,0.9899)) (P=0.016) (Figure 6E), leading to larger spectral gaps and slower mixing rates for spontaneous termination epochs (mean mixing rate termination:0.0089 (95%CI,0.0065,0.0113), sustained:0.012 (95%CI,0.012,0.014); P=0.015) (Figure 6F). The slower mixing of formation and destruction processes also associated with fewer observed numbers of PS in the experimental data (mean sustained: 2.01(95%CI,1.98,2.04),P=0.0109; mean term: 1.83(95%CI,1.42,2.23)) and WF (mean sustained: 2.77(95%CI,2.66,2.88),P=0.0109; mean term: 2.22(95%CI,1.67,2.78)) (Figure 6G-H).

In comparison, mean DF and CL showed no statistically significant differences in sustained versus spontaneously terminating VF (DF: P=0.63; CL: P = 0.78) (Figure 6I-J).

330

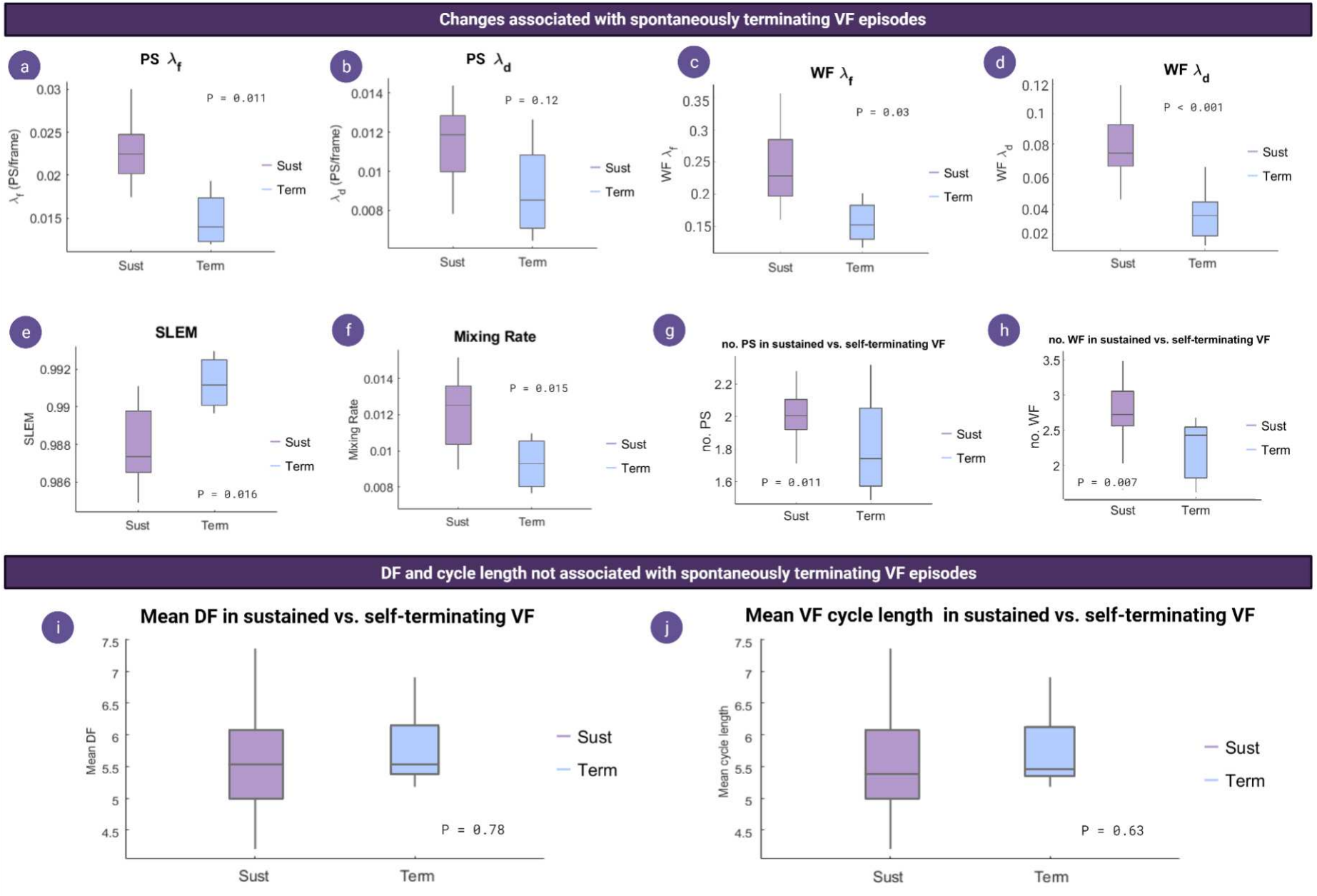
Changes associated with spontaneously terminating VF episodes
a
PS λ_f
λ_f (PS/frame)
P = 0.011
Sust
Term
b
PS λ_d
λ_d (PS/frame)
P = 0.12
c
WF λ_f
WF λ_f
P = 0.03
d
WF λ_d
WF λ_d
P < 0.001
e
SLEM
SLEM
P = 0.016
f
Mixing Rate
Mixing Rate
P = 0.015
g
no. PS in sustained vs. self-terminating VF
no. PS
P = 0.011
h
no. WF in sustained vs. self-terminating VF
no. WF
P = 0.007
DF and cycle length not associated with spontaneously terminating VF episodes
i
Mean DF in sustained vs. self-terminating VF
Mean DF
P = 0.78
j
Mean VF cycle length in sustained vs. self-terminating VF
Mean cycle length
P = 0.63

Figure 6: Observations from spontaneously terminating in human clinical VF episodes

(**6A-D**) Self-terminating VF episodes demonstrated a slower rate of PS formation (PS λ_f, P=0.011), WF formation (WF λ_f, P=0.003), WF destruction (WF λ_d, P<0.001) and PS destruction (PS λ_d, P=0.12) trending towards slowing. (**6E-H**) Self-terminating VF also exhibited larger second largest eigenvalue modulus (SLEM), leading to smaller spectral gaps and slower mixing of formation and destruction processes, indicated by the mixing rate (P<0.05). Overall, this led to fewer numbers of PS and WF in spontaneously terminating VF episodes. (**6F-G**) Mean DF and mean cycle length show no association to spontaneously terminating VF episodes (P>0.05).

Rates of PS formation and destruction increases during the earliest stages of VF, before a period of stabilisation

When analysed by stage (with patient ID set as a random effect), PS λ_f in epochs of sustained human VF demonstrated an abrupt increase during perfusion to ischemia, which slowed during reflow (Figure 7A). This resulted in a temporal intercept of 0.022 (P<0.001). PS λ_d showed a similar trend (temporal intercept = 0.011, P<0.001; Figure 7B). When analysed by time segment (segment lengths= 5sec blocks, with patient ID set as a random effect) PS λ_f and PS λ_d demonstrated the largest increase during the first 15secs of VF (Figure 7C-D), returning a temporal intercept of 0.016 (P<0.001) and 0.008 (P<0.001) respectively.

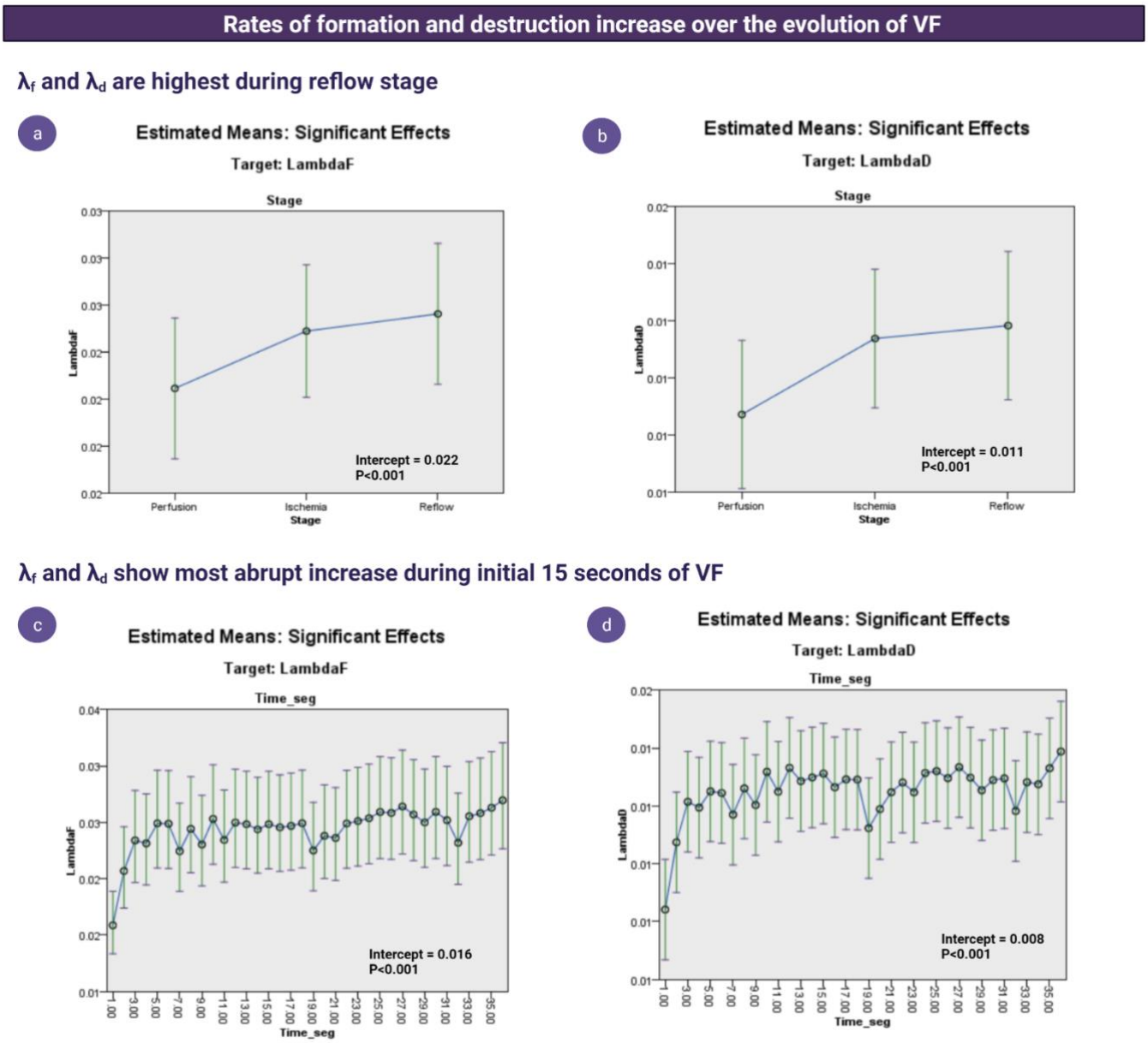

Figure 7: Rates of formation and destruction increase over the evolution of VF

(**7A-B**) Estimated mean charts for significant effects (P<0.05) displayed for λ_f and λ_d when modelled using a generalized linear mixed model by stage (perfusion, ischemia, reflow). (**7C-D**) Estimated mean charts for significant effects for λ_f and λ_d when modelled by time segment (segments = 5sec blocks). λ_f and λ_d increase throughout episodes.

Longest lasting phase singularities are associated with decreased refractoriness

An important area of investigation was the longest-lasting PS likely to be associated with sustained rotational events. To study these events, an extreme value theory approach was implemented (S9). The longest-lasting PS seen during sustained episodes of VF (across all patients and stages of VF) were identified using a generalized extreme value distribution (GED), which gives the distribution of PS lasting over a given threshold, in this case the upper 97.5% percentile of PS lifetimes (1.27sec). Long-lasting PS were then defined as those with the top 5% longest lifetimes from taken from the GED (mean lifetime=1.55sec (95%CI,1.39,2.70), mean number of rotations=10.34 (95%CI, 4.037,16.64)).

Long-lasting PS were found to associate with regions possessing a shorter mean activation interval (AI) (mean AI=201.97ms (95%CI, 187.02, 216.929)), compared to short lasting PS (randomly selected from those lasting >1 rotation, mean lifetime=0.028sec (95%CI,0.003,0.054)) with a mean AI of 231.17 (95%CI, 205.17, 257,16) (P=0.015; Figure 8A-B).

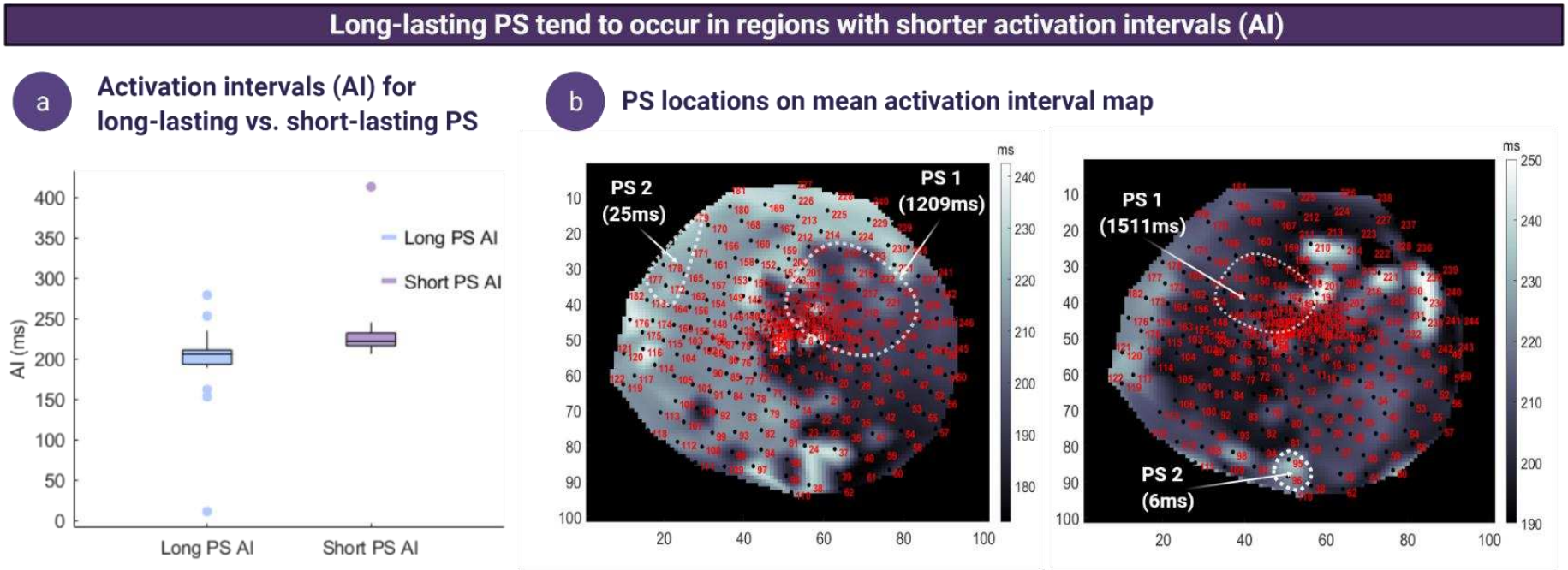

Figure 8: Investigating longest lasting PS

(**8A**) To understand whether sustained PS were associated with differences in refractoriness, the mean activation interval (AI) of sustained versus short-lasting PS was examined. Shorter mean AI were associated with longest lasting PS. (**8B**) Two example AI maps are shown, where longest mean AI in white and shortest in black. Two PS are shown in each AI map. On the left, a sustained PS (PS 1) lasting 1209ms and a short-lasting PS (PS 2) with a lifetime of 25ms is shown. On the right, a sustained PS (PS 1) lasting 1151ms and a short-lasting PS (PS 2) with a lifetime of 6ms is shown.

389 # DISCUSSION

390 ## The M/M/∞ governing equation in human clinical VF

391 A basic property of VF is the continuous regeneration of rotors and wavefronts. Here,
392 we show in human VF that the number and population dynamics of rotors and wavefronts can
393 be modelled with a governing equation derived from an M/M/∞ birth-death process. The M/M/∞
394 equation was found to apply to both short-lasting PS, and sustained PS with lifetimes greater
395 than 1 rotation period. The rate constants of formation and destruction were found to evolve
396 temporally as each epoch progressed, but the M/M/∞ equation was found to apply during all
397 stages of observed VF including perfusion, ischemia and reflow. It was observed that the rate
398 constants of PS formation and destruction trended slower during self-terminating VF episodes
399 compared to those requiring defibrillation, consistent with underlying relative slowing of the VF
400 process as a mechanism to potentially explain spontaneous VF termination.

401 ## Contextualisation in relation to prior cardiac fibrillation research

402 The mechanisms underlying the spatial and temporal organization of VF have long
403 been a source of intensive scientific investigation.[5, 12] The principal advance of the current
404 study is that a common governing equation may potentially regulate the number of rotors and
405 wavefronts in VF. The similarity of this equation between VF and AF[7], provides a unifying link
406 between what have been considered 'different beasts'.[1] This generality may be valuable for
407 understanding fibrillatory mechanisms.

408 One key difference when compared to AF, however, is the observation that PS λ_f and
409 PS λ_d evolve and increase as VF progresses into ischemia before stabilising. Another key
410 difference is that although both PS λ_f and PS λ_d decrease in cases of spontaneously
411 terminating VF, only changes in PS λ_f were statistically significant unlike in AF. Between the
412 model systems, PS λ_f, PS λ_d, WF λ_f and PS WF λ_d in AF are also higher than shown here
413 for VF. This reflects similar previous findings, where an increase in the mapped area led to an
414 increase in the number of PS and WF detected. Consequently, this resulted in new PS and

415 WF formation events being captured more quickly, hence decreasing renewal rates. However,
416 as shown previously an interesting feature of this framework is that these rate constants scale
417 with the size of the mapped area, and that equations apply at each respective scale.[7]

418 Potential mechanistic and clinical applications of the renewal paradigm

419 The current study may assist in providing the foundation for a statistical
420 conceptualisation of fibrillatory dynamics. At the present time there remains ongoing debate
421 about the role of rotors and wavelets as theories of fibrillation.[13, 14] This study suggests that
422 they can conceptualised as probabilistic phenomena arising from a common underlying
423 process.

424 The rate constants derived here could be used to better understand potential structural
425 and electrophysiologic determinants of VF. Recent mechanistic studies posit that VF occurs
426 on a continuous spectrum modulated by factors such as the degree of fibrosis and gap junction
427 coupling.[15] The rate constants could therefore be used to help identify this continuum by
428 providing a single, simple and easily measurable continuous variable that captures how such
429 determinants modulate observed VF dynamics. This would be potentially advantageous
430 compared to postulating that VF is developed by several different mechanisms.

431 Given that episodes of spontaneous VF termination demonstrate slowing of PS and WF
432 formation and destruction process, the rate constants could also provide a potential global
433 therapeutic target that could determine if interventions assist towards achieving VF
434 termination. [16]

435

CONCLUSION

Human VF has complex and disordered dynamics. We present a governing equation to explain the population dynamics of rotors and wavelets in human clinical VF. The governing equation presented here represents the foundation for a statistical paradigm of fibrillatory dynamics with relevance to the field of sudden cardiac death research.

ACKNOWLEDGEMENTS

This work was supported by the National Health and Medical Research Council of Australia Project Grant (1063754) and National Heart Foundation of Australia (101188).

DATA SHARING PLANS

The authors confirm that the code and algorithms used to generate the results within this manuscript will be made available upon request.

REFERENCES

1. Gray R, Jalife JJCAIJoNS. Ventricular fibrillation and atrial fibrillation are two different beasts. Chaos: An Interdisciplinary Journal of Nonlinear Science 1998;8:65-78.
2. Stecker EC, Reinier K, Marijon E, Narayanan K, Teodorescu C, Uy-Evanado A, Gunson K, Jui J, Chugh SSJCA, Electrophysiology. Public health burden of sudden cardiac death in the United States. 2014;7:212-217.
3. Jalife JJArop. Ventricular fibrillation: mechanisms of initiation and maintenance. 2000;62:25-50.
4. Nash MP, Mourad A, Clayton RH, Sutton PM, Bradley CP, Hayward M, Paterson DJ, Taggart PJC. Evidence for multiple mechanisms in human ventricular fibrillation. Circulation 2006;114:536-542.
5. Gray RA, Pertsov AM, Jalife JJN. Spatial and temporal organization during cardiac fibrillation. Nature 1998;392:75-78.
6. Gray RA, Jalife J, Panfilov AV, Baxter WT, Cabo C, Davidenko JM, Pertsov AM, Hogeweg P, Winfree ATJS. Mechanisms of cardiac fibrillation. Science 1995;270:1222-1226.
7. Dharmaprani D, Jenkins E, Aguilar M, et al. M/M/Infinity Birth-Death Processes – A Quantitative Representational Framework to Summarize and Explain Phase Singularity and Wavelet Dynamics in Atrial Fibrillation. Frontiers in Physiology 2021-January-14 2021;11.
8. Dharmaprani D, Schopp M, Kuklik P, Chapman D, Lahiri A, Dykes L, Xiong F, Aguilar M, Strauss B, Mitchell LJCA, Electrophysiology. Renewal theory as a universal quantitative framework to characterize phase singularity regeneration in mammalian cardiac fibrillation. Circulaiton: Arrhythmia and Electrophysiology 2019;12:e007569.
9. Kleinrock L. Queueing systems, volume 2: Computer applications. Vol 66: wiley New York; 1976.
10. Boyd S, Diaconis P, Xiao LJSr. Fastest mixing Markov chain on a graph. 2004;46:667-689.
11. Rogers JMJItobe. Combined phase singularity and wavefront analysis for optical maps of ventricular fibrillation. IEEE transactions on biomedical engineering 2004;51:56-65.
12. Gray RA, Jalife J, Panfilov AV, Baxter WT, Cabo C, Davidenko JM, Pertsov AM, Hogeweg P, Winfree AT. Mechanisms of cardiac fibrillation. Science 1995/11/17/

//1995;270:1222+.

13. Jalife J, Berenfeld O, Mansour MJCr. Mother rotors and fibrillatory conduction: a mechanism of atrial fibrillation. Cardiovascular research 2002;54:204-216.
14. Moe GKJAIPT. On the multiple wavelet hypothesis of atrial fibrillation. Arch Int Pharmacodyn Ther 1962;140:183.
15. Handa BS, Li X, Baxan N, Roney CH, Shchendrygina A, Mansfield CA, Jabbour RJ, Pitcher DS, Chowdhury RA, Peters NSJCr. Ventricular fibrillation mechanism and global fibrillatory organization are determined by gap junction coupling and fibrosis pattern. 2021;117:1078-1090.
16. Hassan T, Jagger C, Barnett DJEMJ. A randomised trial to investigate the efficacy of magnesium sulphate for refractory ventricular fibrillation. 2002;19:57-62.